Journal of Alloys and Compounds 509 (2011) 5769–5772

Contents lists available at ScienceDirect

Journal of Alloys and Compounds

journal homepage: www.elsevier.com/locate/jallcom

Growth and photoluminescence of zinc blende ZnS nanowires via metalorganic chemical vapor deposition

M. Lei [a,*], X.L. Fu [a], P.G. Li [b], W.H. Tang [a]

[a] Faculty of Science, Beijing Univeristy of Posts and Telecommunications, Beijing 100876, China
[b] Department of Physics, Center for Optoelectronics Materials and Devices, Zhejiang Sci-Tech University, Xiasha College Park, Hangzhou 310018, China

ARTICLE INFO

Article history:
Received 4 September 2010
Received in revised form 3 February 2011
Accepted 4 February 2011
Available online 23 February 2011

Keywords:
Semiconductors
Nanostructured materials
Optical property

ABSTRACT

We developed a metalorganic chemical vapor deposition to synthesize ZnS nanowires with high purity on Au-coated sapphire substrates at low temperatures. The ZnS nanowires have zinc blende structure, and most of them have raw-like surface on one edge, while is smooth on the other. High-resolution transmission electron microscopic investigations show that the nanowires are well crystalline single crystal grown along [1 1 1] and are free of bulk defects. The growth mechanism is confirmed as a typical vapor–liquid–solid process. The photoluminescence spectrum reveals two prominent blue emissions centered at 452.2 and 468.6 nm, respectively. It is found that sulfur vacancies and surface states should be responsible for the two blue emissions, respectively.

1. Introduction

As is well known, one dimensional (1D) semiconductor nanowires have attracted considerable attention due to their potential applications in the nanooptics, nanoelectronics and nanomagnetics [1–15]. As an important semiconductor material with wide band gap of 3.72 eV for the zinc blende phase and 3.77 eV for wurtzite phase at room temperature, zinc sulfide (ZnS) has attracted considerable research interest [16–19]. ZnS has been widely used in infrared windows, sensors, lasers, covering electroluminescent devices, and flat panel displays [20–23]. Various methods including conventionally catalytic-assisted thermal evaporation of ZnS powder [24–26], solvothermal process [27,28], and template-assisted electrochemical deposition [29] have been developed to fabricate ZnS nanowires. As is well known, zinc blende crystal structure is more stable than wurtzite up to 1020 °C, and usually exists in bulk form rather than 1D nanostructures [30]. Most of the as-synthesized ZnS nanowires are of metastable wurtzite phase because they are more easily synthesized and formed in metastable 1D nanostructures [31]. Up to now, zinc blende nanowires have been rarely investigated [32–34]. Meng et al. [33] reported a hydrogen-assisted thermal evaporation at elevated temperature as high as 1100 °C. Hu et al. [34] successfully synthesized wurtzite and zinc blende ZnS nanowires. Nevertheless, the as-synthesized nanowires did not have pure phase structure. In this work, we employed a conventional film technique metalorganic chemical vapor deposition (MOCVD) to fabricate well crystalline zinc blende ZnS nanowires grown on sapphire substrates at 530 °C. The microstructure and photoluminescence properties of the zinc blende nanowires were investigated.

2. Experimental

ZnS nanowires were grown on Au-coated sapphire substrates by MOCVD. In the experiment, Au thin films with thickness of 10 nm were sputtered on the sapphire substrates. Diethylzinc and diethylsulphide were used as precursors to supply Zn and S species at flow rates of 0.18 and 7.73 μmol min^{-1}, respectively. High pure hydrogen gas carried the precursors to the substrates at a flow rate of 975 ml/min. Then the reaction chamber was heated quickly to 530 °C and maintained at the peak temperature for 30 min. Finally, the furnace was cooled to room temperature and the products deposited on the sapphire substrates were taken out for further characterization.

The morphology and crystal structure of the products were characterized by field emission scanning electron microscope (FE-SEM, FEI XL30 S-FEG) equipped with energy-dispersive X-ray spectroscopy (EDS) and rotating anode Rigaku (Tokyo, Japan) D/max-2400 X-ray diffractometer with Cu Kα radiation, respectively. The microstructure of the product was investigated by transmission electron microscopy (TEM, Tecnai 20 at 100 kV) and high-resolution TEM (HRTEM, Tecnai 20 at 200 kV). The photoluminescence (PL) spectrum was collected by using the 325 nm line of a He–Cd laser as the excitation source at room temperature.

3. Results and discussion

The morphology and chemical composition of the products deposited on the sapphire substrates were first characterized by SEM. It can be seen from Fig. 1a that highly dense nanowires and a small amount of nanoribbons are distributed over the whole substrates. The magnified SEM image (Fig. 1b) indicates that the

* Corresponding author. Tel.: +86 10 81744637; fax: +86 10 81744637.
E-mail address: leimingiphy@yahoo.com.cn (M. Lei).

0925-8388/$ – see front matter © 2011 Elsevier B.V. All rights reserved.
doi:10.1016/j.jallcom.2011.02.029

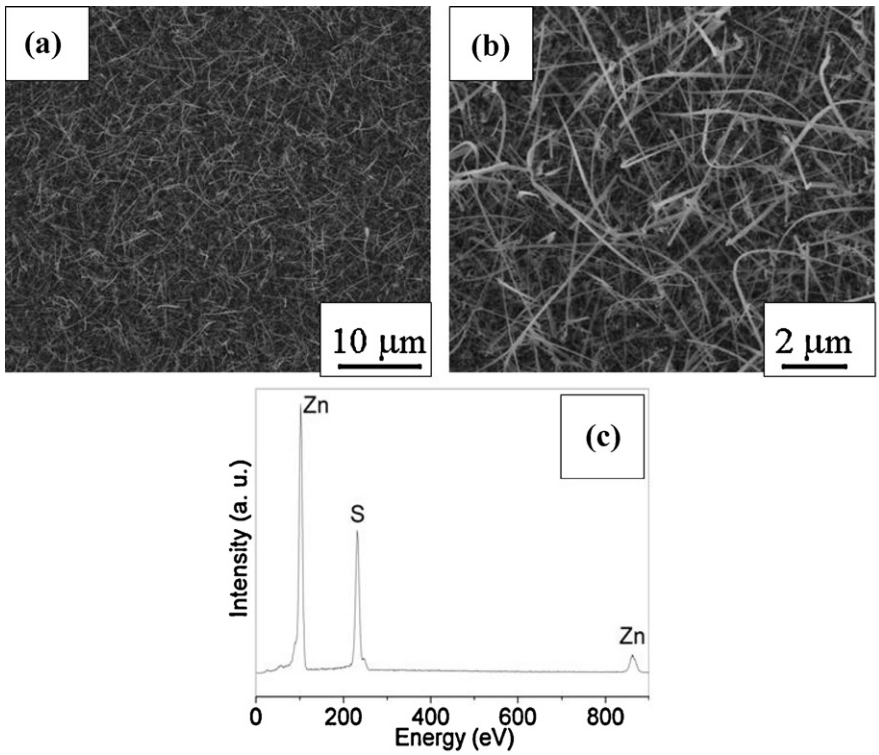

Fig. 1. (a and b) Typical SEM image and magnified SEM image of the deposited products, respectively. (c) EDS spectrum of the deposited products.

length of the nanowires varies from a few micrometers to tens of micrometers, and the diameter is in the range of 80–150 nm. The corresponding EDS spectrum (Fig. 1c) reveals that the nanowires mainly consist of Zn and S elements, and the atom ratio of Zn and S is 1:0.921, close to the stoichiometric ratio of ZnS. The XRD patterns of the nanowires (Fig. 2) can be indexed well on the basis of zinc blende ZnS cell. A small peak in the left side of (1 1 1) peak is also observed. We deduce that it maybe originates from the some impurities. However, the exact impurities cannot be determined and needs to be further investigated. Based on the XRD and EDS measurements, the products are determined as zinc blende ZnS.

Fig. 3a shows TEM image of an individual nanowire, revealing that one edge of the nanowire exhibit saw-like morphology while the other is smooth. The representative saw-like nanowires are *ca.* 70% in the whole nanowires. HRTEM image recorded along [1–10] axis zone (Fig. 3b) shows that the interplanar spacing is 0.32 nm,

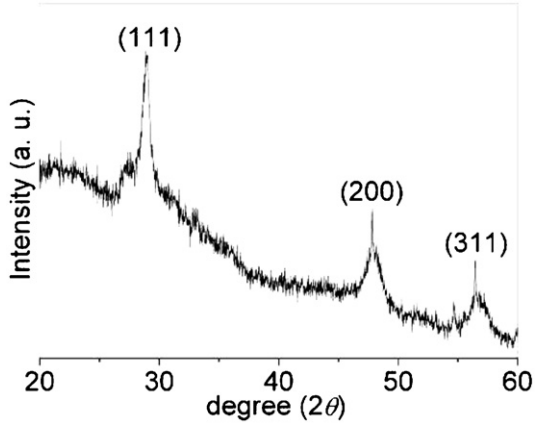

Fig. 2. XRD patterns of the deposited nanowires.

which corresponds to the (1 1 1) planes of zinc blende ZnS, further confirming zinc-blende structure of the nanowire. The corresponding FFT pattern (Fig. 3c) is indexed and reveals well crystalline single-crystal nature of the nanowire. Based on the HRTEM image and FFT pattern, the grow direction is determined as [1 1 1]. Fig. 3d shows TEM image of another nanowire with smooth surfaces. A nanoparticle confirmed as Au catalyst is observed to attach on the tip of the nanowire, suggesting that the growth process follows the well known Au-catalytic vapor–liquid–solid (VLS) mechanism. Epitaxial thin films instead of nanowires are deposited on the substrates without Au catalyst, indicating that Au catalyst plays an important role in the growth of the 1D nanowires. Zhang et al. [35] deduced that Au particles probably acted as the nucleating sites instead of catalyst for ZnSe nuclei because the synthesis temperature of 550 °C is lower than the melting of Au and no catalyst particles are found at the tip of the nanowires. However, we observe that the melting point of Au can be lower below 550 °C at high vacuum or hydrogen atmosphere. In this work, it is found that Au particles can melt below the synthesis temperature of 530 °C and the Au particles on the tip of the straight nanowires (Fig. 3d) are also observed, which indicates that Au acts as catalysts instead of nucleating sites for the nucleation and growth of 1D ZnS nanowires. Au particles can separate from the nanowires after nucleation process, which is rather common in synthesis of other semiconductor nanowires.

Fig. 4 displays the PL spectrum of the ZnS nanowires. Two prominent blue emission bands centered at 452.2 and 468.6 nm, respectively, are detected. PL properties of ZnS nanowires are rather complicated. Various emission bands such as ultraviolet, blue, green, orange and red emission bands, and numerous emission centers had been reported in the previous literatures [28,34,36–40]. It is known from these literatures that emission around 450 nm often are encountered in 1D ZnS nanostructures including nanowires and nanoribbon, and maybe originates from defects e.g., sulfur vacancies and/or bulk defects. Bulk defects such as stacking faults,

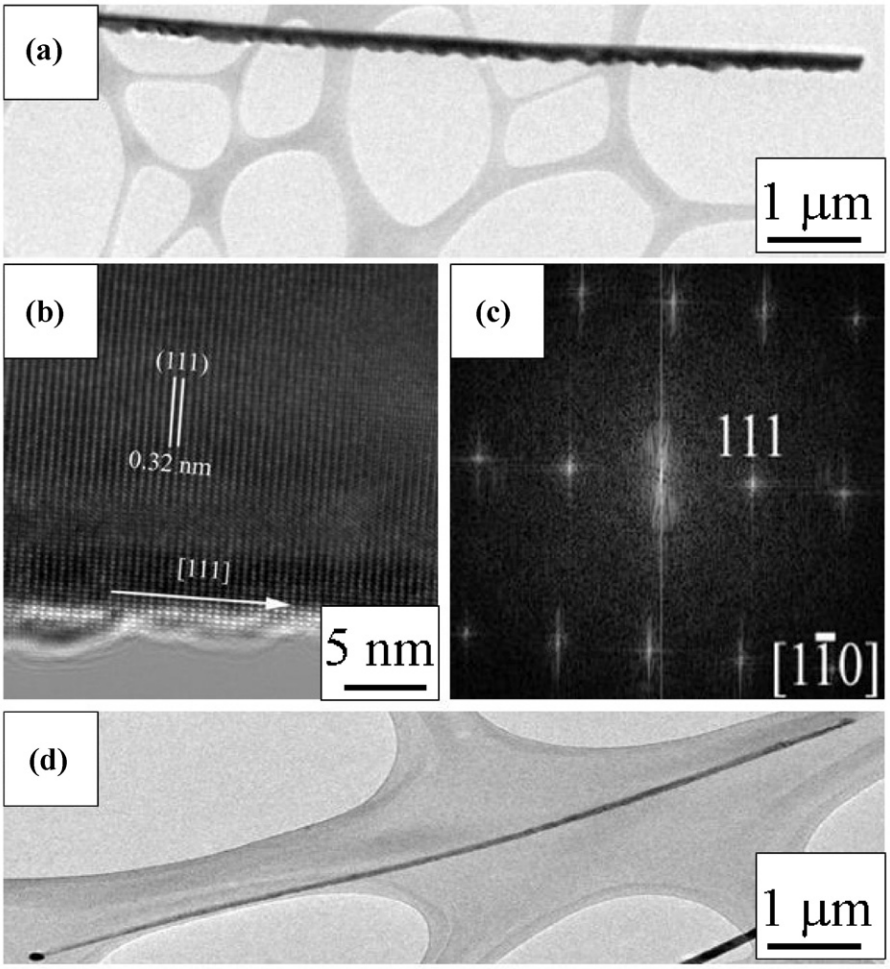

Fig. 3. (a) TEM image of a single ZnS nanowire. (b) HRTEM image of the nanowire. (c) FFT patterns of the nanowire. (d) TEM image of a single nanowire with Au catalyst attached on the tip.

dislocations and twinnings are not detected in the HRTEM image of the nanowires (Fig. 2b). So, we deduce that sulfur vacancy-related point defects are the main reason for the blue emission. According to the donor–acceptor pair recombination mechanism, sulfur vacancies act as the shallow donor species while Zn^{2+} vacancies as the acceptor species. In the case, all carriers excited to the conduction band almost instantaneously decay to shallow donor levels and recombine with acceptor states emitting photons which finally results in the blue emission centered at 452.2 nm here. The blue emission at 468.6 nm is rarely reported. Several literatures [41–43] had reported that various emission bands including white, yellow-orange, orange and blue emissions were detected in metal doped cubic ZnS nanoparticles. The emission bands are different from that observed in this work. The new energy levels and/or particle size, crystallinity, doped situation and surface states may be the main reasons for those emission bands in cubic nanoparticles. Xiong et al. [25] detected the emission band and ascribed it to stoichiometric vacancies or interstitial impurities. But they did not offer exact proof to confirm the explanation. We deduce surface states may be the main reason for the unusual emission because most of the nanowires have raw-like surface on the one edge. However, the exact mechanism is unclear and needs to be further investigated.

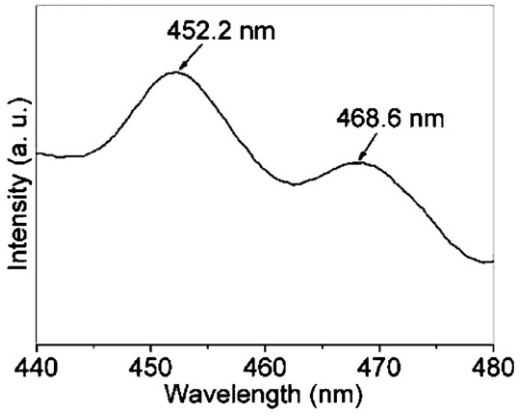

Fig. 4. PL spectrum of the ZnS nanowires.

4. Conclusions

Highly dense ZnS nanowires were fabricated on Au-coated sapphire substrates via a MOVCD method at 530 °C. It is found that the ZnS nanowires have zinc blende structure, which has not been reported before. Most of them have raw-like surface on the one edge, while is smooth on the other. HRTEM measurement indicates that the nanowires are well crystalline single crystal grown along [1 1 1], and bulk defects e.g. stacking faults, dislocations and twinning defects are not detected. The PL spectrum reveals two prominent blue emission bands centered at 452.2 and 468.6 nm, respectively. It is found that donor–acceptor pair recombination between shallow donor associated with sulfur vacancies and Zn^{2+}

vacancies-related acceptor is the main reason for the blue emission centered at 452.2 nm, while surface states should be responsible for the unusual blue emission at 468.6 nm.

Acknowledgements

This work was financially supported by the Innovative Youth Team of Natural Science Foundation of Zhejiang Province (Grant No. R4090058).

References

[1] M. Lei, Q.R. Hu, X. Wang, S.L. Wang, W.H. Tang, J. Alloys Compd. 489 (2010) 663–666.
[2] S.Z. Li, X.D. Ding, J. Li, X.B. Ren, J. Sun, E. Ma, Nano Lett. 10 (2010) 1774–1779.
[3] P.G. Li, Q.R. Hu, W.H. Tang, J. Alloys Compd. 479 (2011) 2776–2779.
[4] A.I. Hochbaum, P.D. Yang, Chem. Rev. 110 (2010) 527–546.
[5] M. Lei, Q.R. Hu, S.L. Wang, W.H. Tang, Mater. Lett. 63 (2009) 1928–1930.
[6] Y.X. Du, F.G. Zeng, J. Alloys Compd. 509 (2011) 1275–1278.
[7] M. Lei, H. Yang, P.G. Li, W.H. Tang, Appl. Surf. Sci. 254 (2008) 1947–1952.
[8] R. Chen, D.H. Li, B. Liu, Z.P. Peng, G.G. Gurzadyan, Q.H. Xiong, H.D. Sun, Nano Lett. 10 (2010) 4956–4961.
[9] H.W. Kim, H.S. Kim, H.G. Na, J.C. Yang, C. Lee, J. Alloys Compd. 500 (2010) 175–180.
[10] M. Lei, H. Yang, P.G. Li, W.H. Tang, J. Alloys Compd. 459 (2008) 338–342.
[11] A.L. Briseno, T.W. Holcombe, A.I. Boukai, E.C. Garnett, S.W. Shelton, J.J.M. Frechet, P.D. Yang, Nano Lett. 10 (2010) 334–340.
[12] H.W. Zhu, P.G. Li, M. Lei, L.H. Li, S.L. Wang, W.H. Tang, J. Alloys Compd. 509 (2011) 3306–3309.
[13] B. Zhang, Y. Jung, H.S. Chung, L.V. Vugt, R. Agarwal, Nano Lett. 10 (2010) 149–155.
[14] F. Shi, D.D. Zhang, C.S. Xue, J. Alloys Compd. 509 (2011) 1294–1300.
[15] F.X. Wu, X.H. Li, Z.X. Wang, H.J. Guo, L. Wu, X.H. Xiong, X.J. Wang, J. Alloys Compd. 509 (2011) 3711–3715.
[16] J. Yan, X.S. Fang, L.D. Zhang, Y. Bando, U.K. Gautam, B. Dierre, T. Sekiguchi, D. Golberg, Nano Lett. 8 (2008) 2794–2799.
[17] X.S. Fang, L.D. Zhang, J. Mater. Sci. Technol. 22 (2006) 721–736.
[18] L.J. Yao, M.J. Zheng, S.H. He, L. Ma, M. Li, W.Z. Shen, Appl. Surf. Sci. 257 (2011) 2955–2959.
[19] L.Y. Yang, W.J. Wang, B. Song, R. Wu, J. Li, Y.F. Sun, F. Shang, X.L. Chen, J.K. Jian, J. Crystal Growth 312 (2010) 2852–2856.
[20] J.F. Xu, W. Ji, J. Mater. Sci. Lett. 18 (1999) 115–117.
[21] L. Sun, C. Liu, C. Liao, C. Yan, J. Mater. Chem. 9 (1999) 1655–1657.
[22] T.V. Prevenslik, J. Lumin. 87–89 (2000) 1210–1212.
[23] G.Z. Shen, Y. Bando, D. Golberg, Appl. Phys. Lett. 88 (2006) 123107.
[24] S. Kar, S. Chaudhuri, J. Phys. Chem. B 109 (2005) 3298–3302.
[25] Q.H. Xiong, G. Chen, J.D. Acord, X. Liu, J.J. Zengel, H.R. Gutierrez, J.M. Redwing, L.C. Lew Yan Voon, B. Lassen, P.C. Eklund, Nano Lett. 4 (2004) 1663–1668.
[26] X.S. Fang, Y. Bando, C.H. Ye, G.Z. Shen, D. Golberg, J. Phys. Chem. C 111 (2007) 8469–8474.
[27] G.C. Xi, C. Wang, X. Wang, Q. Zhang, H.Q. Xiao, J. Phys. Chem. C 112 (2008) 1946–1952.
[28] H.M. Wang, Z. Chen, Q. Cheng, L.X. Yuan, J. Alloys Compd. 478 (2009) 872–875.
[29] M. Chang, X.L. Cao, X.J. Xu, L.D. Zhang, Phys. Lett. A 372 (2008) 273–276.
[30] Z.W. Wang, L.L. Daemen, Y.S. Zhao, C.S. Zha, R.T. Downs, X.D. Wang, Z.L. Wang, R.J. Hemley, Nature Mater. 4 (2005) 922–927.
[31] L.W. Yin, Y. Bando, Nature Mater. 4 (2005) 883–884.
[32] H.X. Chen, D.N. Shi, J.S. Qi, J.M. Jia, B.L. Wang, Phys. Lett. A 373 (2009) 371–375.
[33] X.M. Meng, J. Liu, Y. Jiang, W.W. Chen, C.S. Lee, I. Bello, S.T. Lee, Chem. Phys. Lett. 382 (2003) 434–438.
[34] J.T. Hu, G.Z. Wang, C.X. Guo, D.P. Li, L.L. Zhang, J.J. Zhao, J. Lumin. 122–123 (2007) 172–175.
[35] X.T. Zhang, K.M. Ip, Z. Liu, Y.P. Leung, Q. Li, S.K. Hark, Appl. Phys. Lett. 84 (2004) 2641–2643.
[36] W.T. Yao, S.H. Yu, L. Pan, J. Li, Q.S. Wu, L. Zhang, J. Jiang, Small 1 (2005) 320–325.
[37] Y. Yang, W.J. Zhang, Mater. Lett. 58 (2004) 3836–3838.
[38] G.Z. Shen, Y. Bando, D. Golberg, J. Phys. Chem. B 110 (2006) 20777–20780.
[39] Z.X. Zhang, J.X. Wang, H.J. Yuan, Y. Gao, D.F. Liu, L. Song, Y.J. Xiang, X.W. Zhao, L.F. Liu, S.D. Luo, X.Y. Dou, S.C. Mou, W.Y. Zhou, S.S. Xie, J. Phys. Chem. B 109 (2005) 18352–18355.
[40] C.S. Tiwary, P. Kumbhakar, A.K. Mitra, K. Chattopadhyay, J. Lumin. 129 (2009) 1366–1370.
[41] B.H. Dong, L.X. Cao, G. Su, Q. Wei, H. Zhai, J. Alloys Compd. 492 (2010) 363–367.
[42] X.D. Lü, J. Yang, Y.Q. Fu, Q.Q. Liu, B. Qi, C.L. Lü, Z.M. Su, Nanotechnology 21 (2010) 115702.
[43] R. Sarkar, C.S. Tiwary, P. Kumbhakar, P. Basu, A.K. Mitra, Physica E 40 (2008) 3115–3120.